PROTEINS: Structure, Function, and Genetics 5:271–280 (1989)

Three-Dimensional Structure of a Fluorescein–Fab Complex Crystallized in 2-Methyl-2,4-pentanediol

James N. Herron,[1] Xiao-min He,[1] Martha L. Mason,[1] Edward W. Voss, Jr.,[2] and Allen B. Edmundson[1]
[1]Department of Biology, University of Utah, Salt Lake City, Utah 84112 and [2]Department of Microbiology, University of Illinois, Urbana-Champaign, Illinois 61081

ABSTRACT **The crystal structure of a fluorescein–Fab (4-4-20) complex was determined at 2.7 Å resolution by molecular replacement methods. The starting model was the refined 2.7 Å structure of unliganded Fab from an autoantibody (BV04-01) with specificity for single-stranded DNA. In the 4-4-20 complex fluorescein fits tightly into a relatively deep slot formed by a network of tryptophan and tyrosine side chains. The planar xanthonyl ring of the hapten is accommodated at the bottom of the slot while the phenylcarboxyl group interfaces with solvent. Tyrosine 37 (light chain) and tryptophan 33 (heavy chain) flank the xanthonyl group and tryptophan 101 (light chain) provides the floor of the combining site. Tyrosine 103 (heavy chain) is situated near the phenyl ring of the hapten and tyrosine 102 (heavy chain) forms part of the boundary of the slot. Histidine 31 and arginine 39 of the light chain are located in positions adjacent to the two enolic groups at opposite ends of the xanthonyl ring, and thus account for neutralization of one of two negative charges in the haptenic dianion. Formation of an enol-arginine ion pair in a region of low dielectric constant may account for an incremental increase in affinity of 2–3 orders of magnitude in the 4-4-20 molecule relative to other members of an idiotypic family of monoclonal antifluorescyl antibodies. The phenyl carboxyl group of fluorescein appears to be hydrogen bonded to the phenolic hydroxyl group of tyrosine 37 of the light chain. A molecule of 2-methyl-2,4-pentanediol (MPD), trapped in the interface of the variable domains just below the fluorescein binding site, may be partly responsible for the decrease in affinity for the hapten in MPD.**

Key words: antifluorescyl monoclonal antibody, high-affinity binding site, effects of MPD on hapten binding

INTRODUCTION

The antifluorescein system is well suited for studying the molecular basis of antigenic specificity because it offers both a wide range of binding affinities (10^5–10^{10} M^{-1}), and a variety of experimental techniques for correlating antigen binding affinities, kinetics, and thermodynamics.[1–9] Furthermore, it has been possible to develop a family of idiotypically cross-reactive antibodies in which individual monoclonals vary in affinity over a 1000-fold range.[9] Amino acid sequences recently determined for eight of these antibodies in one of our laboratories (E.W.V.) show that at least six were derived from the same germline variable genes. Thus, the antifluorescein idiotype family can be used to further the understanding of both idiotypy and affinity maturation. In this report, we describe the three-dimensional structure of a complex of dianionic fluorescein with the antigen-binding fragment from the antibody (4-4-20) with the highest affinity in this idiotype family.

The 4-4-20 monoclonal is an IgG_{2a} (κ) antibody that binds fluorescein with an association constant of 3.4×10^{10} M^{-1} in aqueous solution. This affinity decreases 300-fold in 47% (v/v) 2-methyl-2,4-pentanediol (MPD), the solvent used for cocrystallization of the 4-4-20 Fab with fluorescein hapten.[5] The antibody is a highly specialized molecule that does not cross-react with rhodamine compounds.[1,6] In the formation of a complex with the 4-4-20 antibody, fluorescein satisfied criteria for a site-filling ligand, with the xanthonyl ring behaving as the "immunodominant" moiety.[6] Despite its relatively large size and distinctive chemical features, fluorescein induces a diverse immune response when injected as a conjugate with keyhole limpet hemocyanin (KLH).[1,7–9] Interpretation of binding studies have sometimes been ambiguous with heterogeneous populations of antibodies. It therefore seemed appropriate to determine the mode of binding in a single molecular species, particularly one with high affinity for fluorescein.

This crystal system affords a rare opportunity to consider both the structural features responsible for high-affinity binding and the effects of solvent in lowering that affinity. The complex will also be ex-

Received January 20, 1989; revision accepted March 24, 1989.

Address reprint requests to A.B. Edmundson, Department of Biology, University of Utah, Salt Lake City, UT 84112.

James N. Herron's present address is Department of Pharmaceutics, University of Utah, Salt Lake City, UT 84112.

amined to assess the influence of the carrier protein (KLH) on the location and orientation of the hapten in the combining site. In the preparation of the immunogen, molecules of the isothiocyanate derivative of fluorescein amine (isomer I) were coupled to KLH, with the principal reactions presumed to involve the ϵ-amino group of lysine side chains. The 4-4-20 hybridoma was obtained by fusion of hyperimmune splenocytes stimulated with the fluorescein–KLH conjugate.

The present work adds to previous crystallographic studies of complexes in which small molecules were diffused into crystals of human and murine immunoglobulin fragments with binding sites shaped like cavities or shallow depressions.[10–15] These studies have helped define the molecular basis of low- and medium-affinity interactions and have provided the background to broaden our understanding of antigenic specificity. Block-end types of interactions over large external surfaces have been studied in cocrystals of Fab molecules and protein antigens like lysozyme and influenza neuraminidase.[16–19] Antibodies binding DNA have grooves as potential combining sites, and cocrystals of Fabs and oligodeoxynucleotides are currently being subjected to X-ray analyses.[20–23] The structure of an unliganded Fab (J539) with specificity for galactan in carbohydrates has also been determined.[24] A model for the binding of the ligand was proposed on the basis of solution studies and the structure of the combining site.

Recently, a single-chain antigen-binding protein[25] was constructed to simulate the Fv fragment of the 4-4-20 antibody (an Fv fragment consists of the "variable" domains of the heavy and light chains). The three-dimensional structure of the 4-4-20 Fab should prove very useful in assessing the properties and applications of the single chain protein.

MATERIALS AND METHODS

Preparation of Fluorescein–Fab Complex

Procedures for the isolation and purification of the 4-4-20 monoclonal antibody and fluorescein–Fab complex were described in a previous article.[5] In outline the Fab fragments were prepared by hydrolysis of fluorescein–IgG complexes with papain. Liganded Fabs were purified by chromatofocusing on 15 ml Pharmacia PBE 94 columns, with a linear pH gradient of 9 to 6 formed with Pharmacia Polybuffer 96. Because of potential destructive effects of dye-sensitized photooxidation by free fluorescein, it was necessary to protect the liganded protein from light at all stages of the procedures. Columns, tubes, and vessels used in affinity chromatography, chromatofocusing, dialysis, enzymatic hydrolysis, and crystallization trials were all covered with aluminum foil. All manipulations and transfers were carried out in reduced light. Under such precautions the liganded Fab was eluted from the chromatofocusing column as a single component with a p*I* of 7.2.

After dialysis against 50 mM sodium phosphate, pH 7.2, the solution of the fluorescein–Fab complex was concentrated to 25 mg/ml by ultrafiltration (the acceptable range for crystallization was 10–30 mg/ml). The complex was crystallized by a batch method in an environment with strict light and temperature (12–14°C) control. Graded aliquots of MPD were added to 40 μl samples of the liganded protein in flat-bottomed glass vials. Crystals appeared in 2 days with final MPD concentrations of 38–60% (v/v), the optimum being ~47%. Bladed crystals suitable for X-ray analysis grew to dimensions of 0.6 × 0.35 × 0.3 mm (l × w × d) in 1–2 months. Green fluorescence, attributable to the dissociation of fluorescein from the complex in MPD, was observed in each crystallization tube.

Collection of X-Ray Diffraction Data

The fluorescein–Fab complex crystallized in the triclinic space group *P*1, with $a = 58.3$, $b = 43.9$, and $c = 42.5$ Å; $\alpha = 82.1$, $\beta = 87.3$, and $\gamma = 84.6°$.[5] Crystals disintegrated at temperatures >22°C, but were mechanically stable even in the X-ray beam when the ambient temperature was maintained at 12–14°C. Temperature instability of the complex in MPD had also been noted in solution.[5] For example, irreversible increases in the standard free-energy changes ($\Delta G°$) in the liganded IgG and Fab molecules occurred in 40% MPD at relatively low temperatures (transition temperature of 30°C).

A single crystal was used to collect X-ray diffraction data to 2.7 Å resolution with a Nicolet P21 diffractometer operated at 40 kV and 35 mA (CuK_α radiation). The data set included 11,116 unique reflections, of which 9120 (82.0%) were observed at intensity levels >1.5 standard deviations (based on counting statistics).

Determination of the Three-Dimensional Structure of the Liganded Fab

The fluorescein–Fab complex crystallized in the same space group (*P*1) as the unliganded Fab of the BV04-01 IgG_{2b} autoantibody, with specificity for single-stranded DNA.[5,26] Unit cell dimensions for the two crystals were nearly identical and one of us (X-M.H.) found by molecular replacement methods[27–30] that the proteins were in the same orientations in these unit cells. With the refined 2.7 Å structure of the BV04-01 Fab as starting model, the orientation of the 4-4-20 Fab was determined more accurately with rotation function programs.

Crystallographic refinement[31,32] of the structure was initiated with the X-ray diffraction data[5] for the 4-4-20 Fab and the atomic model of the BV04-01 Fab.[22,23] After 30 cycles of refinement with 2.7–6.0 Å data (8304 reflections), the amino acid sequences

TABLE I. Refinement Data

	Actual rms deviation	Target value
Average ΔF*	46.6	
R-factor	0.215	
$< B >$ in Å^2†	15.5	
No. of reflections, $I > 1.5\ \sigma\ (I)$‡	8304	
Root mean square (rms) deviations		
From ideal distance (Å)		
Bond distance	0.028	0.03
Angle distance	0.055	0.04
Planar 1-4 distance	0.032	0.03
Hydrogen bond distance§	0.132	0.05
rms deviation from planarity (Å)	0.014	0.025
rms deviation from ideal chirality (Å^3)	0.210	0.150
rms deviation from permitted contact distances (Å)		
Single torsion contacts	0.280	0.500
Multiple torsion contacts	0.400	0.500
Possible hydrogen bond	0.409	0.500
rms deviation from ideal torsion angles (°)		
For prespecified ϕ, ψ angles	30.8	15.0
For planar group (0 or 180)	6.3	3.0
For staggered group (± 60 or 180)	26.9	15.0
For orthonormal group (± 90)	28.1	15.0

*The weight for the structure factor refinement was obtained from the equation $\omega = (1/\sigma)^2$, where $\sigma = 40 - 278 \times [\sin(\theta)/\lambda - 1/6]$.
†Average temperature factor.
‡Resolution limits of 2.7–6.0 Å.
§Explicit hydrogen bonds for β-pleated sheets.

of the light and heavy chains were altered to correspond to those of the 4-4-20 Fab.[34] The model of the 4-4-20 Fab was improved through alternating cycles of refinement and interactive model building on an Evans and Sutherland PS300 graphics system with the FRODO program.[35,36] Polypeptide backbones and amino acid side chains were fitted to $2F_o-F_c$ maps, in which F_o and F_c were observed and calculated structure factors. Fluorescein was located in a ΔF (F_o-F_c) map, for which the phase angles were calculated from the refined atomic model of the protein (atomic coordinates for fluorescein were omitted). The ligand–protein complex was subjected to additional cycles of refinement until the R factor ($\Sigma \| F_o | - | F_c \| / \Sigma | F_o |$) began to plateau at its current value of 0.180 (before idealization of bond lengths and angles; 0.215 after).

RESULTS

Description of the Three-Dimensional Structure of the Fluorescein–Fab Complex

The results of the crystallographic refinement of the complex are presented in Table I. This structure could be refined very quickly because of the great similarities with the structure of the unliganded BV04-01 Fab.

Figure 1 contains the three-dimensional "cage" electron density to which a skeletal model of fluorescein was fitted by interactive computer graphics. The torsion angle measured between the xanthonyl and benzoyl rings was 73° in the bound hapten.

An αC skeletal model of the 4-4-20 Fab is shown as a stereo pair in Figure 2, with a model of fluorescein codisplayed in the binding site. Tracings of the αC chains of the 4-4-20 and BV04-01 Fabs are superimposed in Figure 3. Details of the structures of the ligand and combining site are presented in Figure 4 (skeletal models). Solvent-accessible surfaces[37] are illustrated in Figure 5. Amino acid sequences[34] for the hypervariable regions are listed in Figure 6.

Polypeptide chains could be traced unambiguously in both the light and heavy chains of the 4-4-20 complex. Significantly, the third hypervariable loop, which was difficult to follow in the heavy chain of the BV04-01 Fab, was well defined in the fluorescein–Fab complex. In the presence of ligand, constituents of this loop were found to have small temperature factors (B values), characteristic of regions with low mobility.

Comparison of the Structures of the 4-4-20 and BV04-01 Fabs

The 4-4-20 Fab is an extended molecule in which the pseudotwofold axes between the pairs of variable and constant domains are nearly colinear (i.e., the measured "elbow bend" angle between the two pseudodiads is 171°). Except for the third hypervariable loops, in which the 4-4-20 heavy chain is shorter than the BV04-01 sequence by three residues, the αC tracings are remarkably similar in the two proteins. This similarity is readily understand-

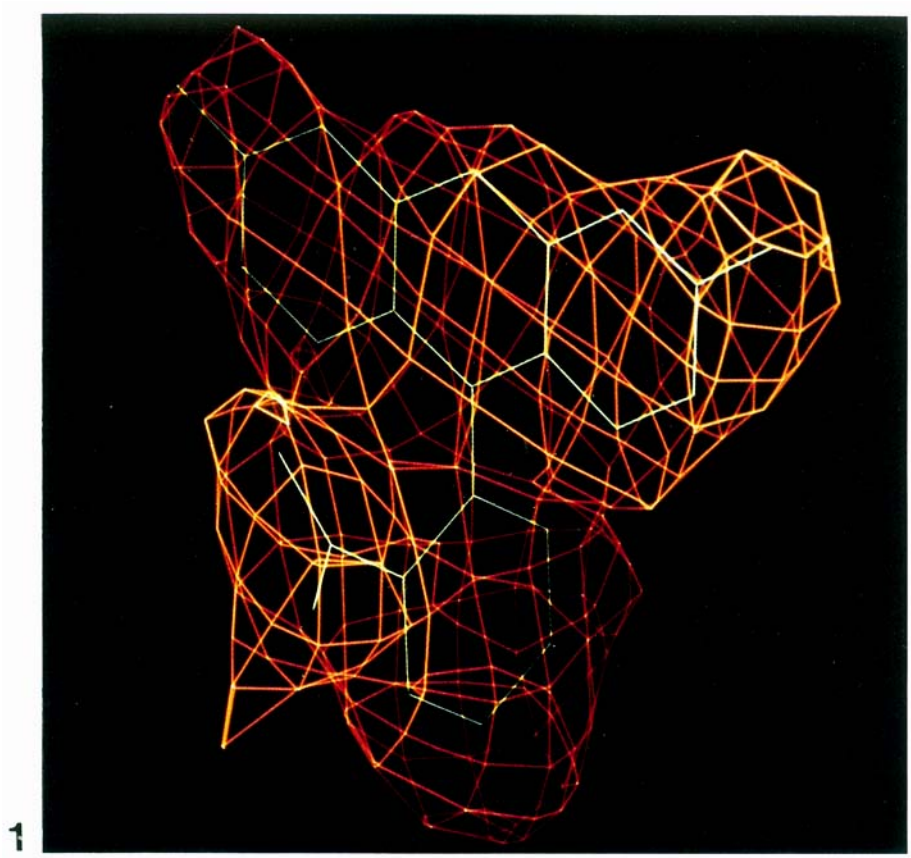

Fig. 1. Three-dimensional electron density (orange) corresponding to fluorescein (green) in the combining site of the 4-4-20 Fab. This electron density was obtained in a difference Fourier map after crystallographic refinement of the ligand–protein complex. A skeletal model of fluorescein was fitted to the electron-density by interactive computer graphics.

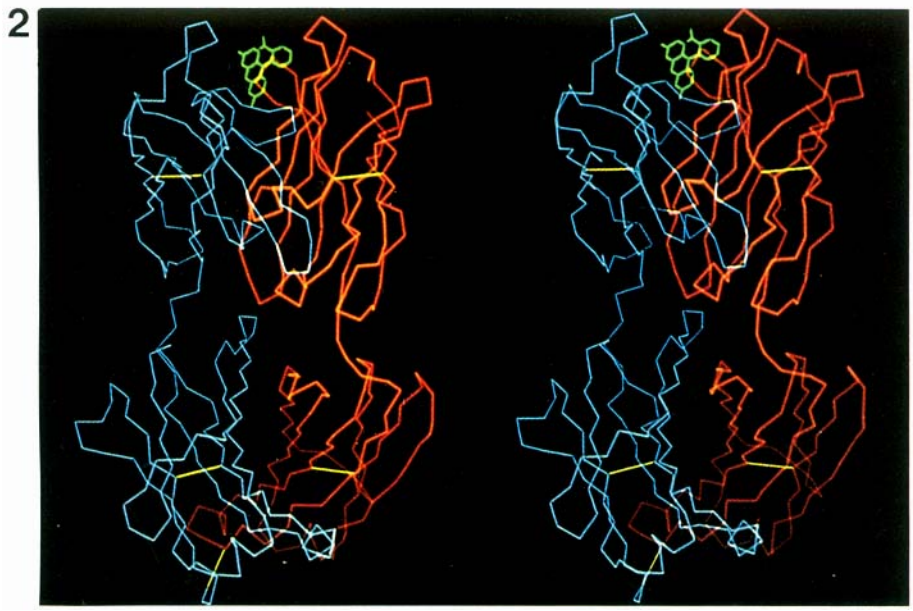

Fig. 2. Stereo diagram of α C tracings of the light (blue) and heavy (red) chains of the 4-4-20 Fab, with fluorescein (green) in the combining site. The "variable" domains are at the top and the "constant" domains are at the bottom. Disulfide bonds are represented by yellow bars.

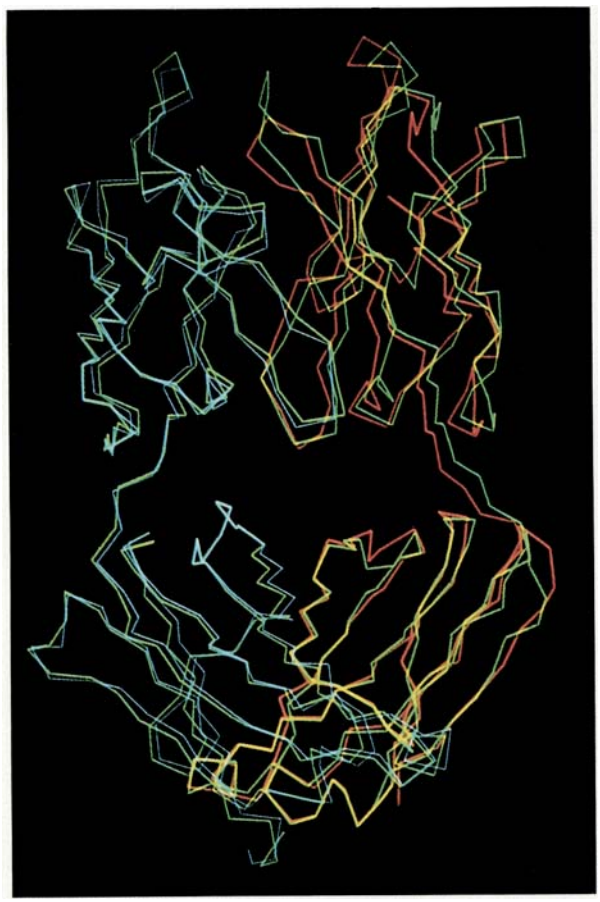

Fig. 3. Superimposed αC tracings of the 4-4-20 and BV04-01 Fabs, the latter having specificity for single-stranded DNA. The two chains of the 4-4-20 Fab are colored red (heavy) and blue (light). The 4-4-20 Fab was cocrystallized with fluorescein in 2-methyl-2,4-pentanediol and the BV04-01 Fab was crystallized without ligand in ammonium sulfate. Yet the two crystals were nearly isomorphous and the structures of the Fabs were very similar.

able in the light chains, which differ in only six amino acid positions.[34] However, there are 42 replacements in the variable domain of the 4-4-20 heavy chain. Substitutions that appear to be critical for the binding of fluorescein are arginine 39 for histidine and tryptophan 101 for leucine in the light chain; tryptophan 33 for alanine and glutamine 50 for arginine in the heavy chain. Because of differences in the lengths of the third hypervariable loops, tyrosine 102 and 103 have no direct counterparts in the BV04-01 Fab. Interestingly, arginine 39 is replaced by histidine in other members of the antifluorescyl idiotype family and by glutamine in the Mcg Bence–Jones dimer. This glutamine is located outside the regions available for ligand binding.[12]

Fluorescein Binding Site

Fluorescein fits into a slot lined by constituents of both the light and heavy chains (see Figs. 4 and 5), and participates in a network of interacting aromatic groups with the protein. There are 68 pairs of atoms of the ligand and protein separated by <4 Å. Of the potential interactions, 42 are associated with the xanthonyl moiety and 26 with the benzoyl group of fluorescein. This distribution is consistent with the assignment of the xanthonyl moiety as the "immunodominant" portion of the hapten.

Tryptophan L101 forms the bottom of the slot and tryptophan H33 and tyrosine L37 provide the sides. The width of the slot, as measured from the distance between the centroids of the rings of tryptophan H33 and tryosine L37, is about 9 Å. The phenolic ring of tyrosine L37 is stacked with the xanthonyl moiety of fluorescein. Tryptophan H33 interacts with the hapten to produce an aromatic pair of the type described by Burley and Petsko.[38] One enolic group (oxygen 1) on the xanthonyl ring is only 3.0 Å from an imidazolium nitrogen of histidine L31. The other enolic group (oxygen 3) is sufficiently close (2.8 Å) to the guanido group of arginine L39 for an electrostatic interaction and is also within hydrogen bonding distance of serine L96. Thus one of the ligand's two negative charges is neutralized by the antibody. Oxygen 2, in the ether linkage at the top of the middle ring of the xanthonyl moiety, does not participate in interactions with the protein.

Surprisingly, the second negative charge on fluorescein (the carboxylic acid) is not formally neutralized by a protein substituent. Instead, this group faces the solvent at an open end of the slot. Partial charge compensation is achieved by the formation of a hydrogen bond between the phenolic hydroxyl group of tyrosine L37 and one of the carboxylic acid oxygen atoms (the electron density in a $2F_o-F_c$ map is continuous between the two sets of atoms).

Tyrosine 103 extends toward the phenyl ring of fluorescein and tyrosine 102 contributes to the structural integrity of the binding site without actually being in contact with the hapten (see Fig. 4). There is a clear solvent channel for a lysine side chain to be connected to an isothiocyanate group in the para position of the phenyl ring, as would be expected for a hapten coupled to the KLH carrier protein in the immunogen. This solvent channel is shown in Figure 5.

Glutamine H50, which replaces an important arginine residue in the putative binding site of the BV04-01 Fab, is mostly buried in the presence of fluorescein in the 4-4-20 Fab. However, the polar end of the side chain (the carbonyl oxygen of the amide group) is within hydrogen bonding distance of the indole nitrogen of tryptophan H33. Arginine H52, another key residue in the BV04-01 binding region, is salt bridged to glutamic acid H59 (an alanine in BV04-01).

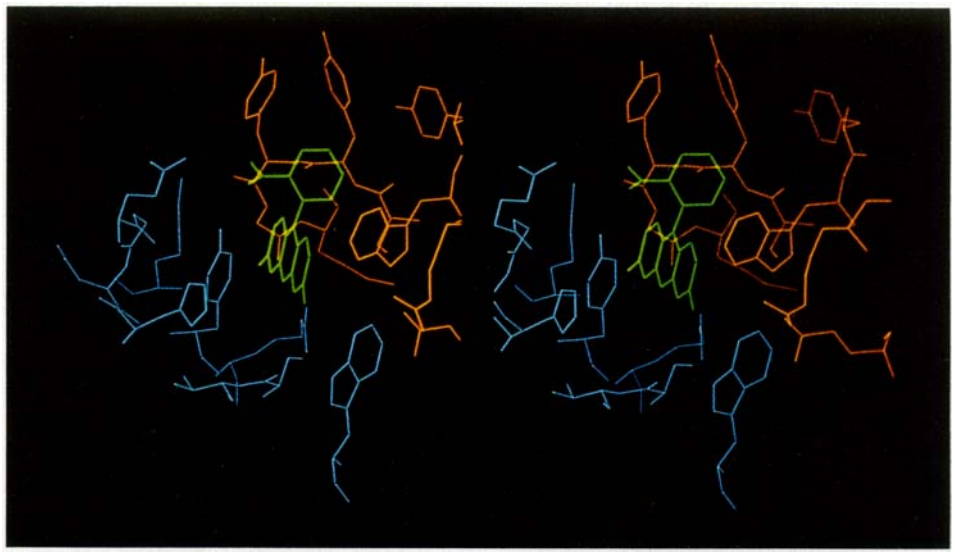

Fig. 4. Stereo diagram of the hapten binding site in the 4-4-20 Fab. Light (L) chain constituents are blue, heavy (H) chain components are red, and fluorescein is green. The xanthonyl (three ring) group of fluorescein is flanked by tyrosine L37 on the left and tryptophan H33 on the right, with tryptophan L101 forming the bottom of the slot. Enolic oxygen atoms on opposite corners of the xanthonyl group point toward histidine L31 (left) and arginine L39 (right). The phenyl carboxyl group of fluorescein (single ring) is located below tyrosines H103 (left) and H102 (right).

Fig. 5. Solvent-accessible surface dot representation[37] of the hapten combining site, with a skeletal model of fluorescein superimposed. Note the free space above the para position of the phenylcarboxyl group of fluorescein. In the immunogen used to elicit the production of the 4-4-20 antibody, a lysine side chain on a carrier protein would be linked to an isothiocyanate group in the para position of the hapten. Lysine would presumably occupy the free space when the hapten entered the antibody combining site.

Crystal Packing Interactions in the 4-4-20 and BV04-01 Systems

Analyses of packing interactions revealed structural features that are conducive to the formation of 4-4-20 Fab crystals nearly isomorphous with those of the unliganded BV04-01 Fab. Light chain constituents of the 4-4-20 Fab were found to be involved in a large proportion (23 of the 26 examples in the survey) of major packing interactions. The light chain is also prominent in crystal packing of the unliganded BV04-01. The close similarities in amino acid sequences and conformations of the two light chains are apparently reflected in the packing of the parent Fabs, despite the differences in crystallizing media.

Sequestering of an MPD Molecule in the V_L–V_H Interface

In the interface of the variable domains below the fluorescein binding site (closest distance ~4.6 Å), there was a module of electron density that could not be assigned to either protein or hapten. This module had the size and shape expected for a molecule of MPD, and persisted in maps calculated after advanced stages of the crystallographic refinement.

The cage electron density for the putative solvent molecule is shown with the surrounding protein constituents in Figure 7. MPD was omitted from the model used to calculate the phases for the difference Fourier map. The binding site for MPD was lined by both polar and apolar residues, such as threonine 99, serine 101, and tryptophans 47 and 108 of the heavy chain, and arginine 39, tyrosine 41, and tryptophan 101, and phenylalanine 103 of the light chain. Hydroxyl groups on threonine H99 and tyrosine L41 were located within hydrogen bonding distances of the 2- and 4-hydroxyl groups of MPD.

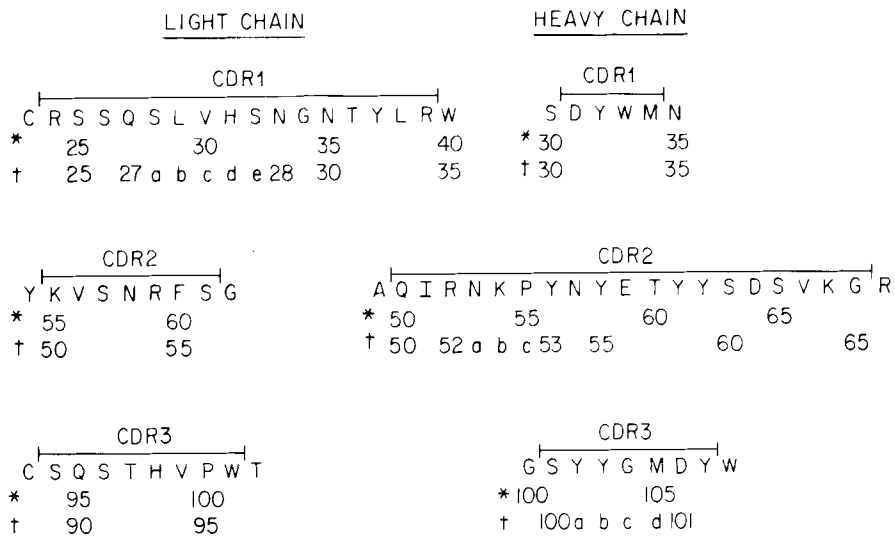

Fig. 6. Amino acid sequences of the hypervariable regions (complementarity-determining regions or CDR[45]) of the light and heavy chains of the 4-4-20 Fab. These sequences were determined by Bedzyk et al.[34] (*) The strict sequential numbering system used in our computers and graphics terminals. (†) The more widely used numbering scheme of Kabat et al.[45]

DISCUSSION

A simple, yet restricted combining site seems well suited for a specialized high-affinity antibody for fluorescein. Space available for binding in the site is limited. While geometrically optimized, the aromatic, electrostatic, and hydrogen bonding interactions are relatively few in number. We suspect that the formation of such a tight complex was accompanied by conformational adjustments in the protein. Recent immunological studies support this view. For example, antibodies elicited to the liganded site of the 4-4-20 antibody were not reactive with the nonliganded, idiotypic state.[39] These studies suggest the generation of new epitopes on ligand binding as a consequence of induced conformational changes.

It is interesting to ask what factors contribute to a high-affinity site. There is a red shift in the absorption spectrum when fluorescein is bound to the 4-4-20 and other monoclonal antifluorescyl antibodies.[2,40] This shift has been attributed to hydrophobic effects involving tryptophan side chains. The model of the complex supports such a view, since two trytophan residues are located in close juxtaposition to the ligand in the 4-4-20 combining site. However, strategically placed tryptophans are not sufficient to account for the high affinity of 4-4-20. For example, the 9-40 antifluorescyl antibody has tryptophan residues in homologous positions in its amino acid sequence and a lower affinity for the ligand than 4-4-20.[41]

Quenching of fluorescence is characteristic of antifluorescyl antibodies. The maximum quenching constant for the 4-4-20 molecule is greater than the Q_{max} values of some antibodies (e.g., 20-4-4), but slightly smaller than those for other antibodies (e.g., 20-20-3) with lower affinities for fluorescein.[2,40] Moreover, Q_{max} for 4-4-20 actually increases in MPD while the ligand affinity decreases.[5] These results indicate that there is not a strong correlation between fluorescence quenching and high affinity. Interactions resulting in quenching appear to be very diverse. Tryptophan has been invoked as a possible participant in such interactions and in one case (20-20-3) histidine was suggested to be involved in the protonation of the enolic group of bound fluorescein.[2] The 4-4-20 active site contains both tryptophan and histidine residues in positions that should be favorable for fluorescence quenching.

Model-based hypotheses seem to be especially useful in explaining deuterium fluorescence enhancement[2,42] and iodine quenching[43] of bound ligand in antifluorescyl antibodies. The liganded 4-4-20 molecule shows about 188% fluorescence enhancement in deuterium oxide (relative to water). Such experiments afford a measure of the degree of hydrogen bonding between ligand and protein. The enhancement for 4-4-20 was 10 times greater than values for four other antifluorescyl monoclonal antibodies and hydrogen bonding was therefore considered to be very important for ligand binding.[2] The structure of the complex is consistent with this proposal and can be used to identify the most prominent hydrogen bonds (enol with histidine L31 and phenyl carboxyl group with tyrosine L37). Only 2.5% quenching of bound fluorescein was noted when the liganded 4-4-20 IgG was titrated with potassium iodide.[9,43] This observation indicated that fluorescein bound in the 4-4-20 active site was essentially inaccessible to iodide. Quenching was higher (8.4–15.5%) in four other antibodies with lower affinities

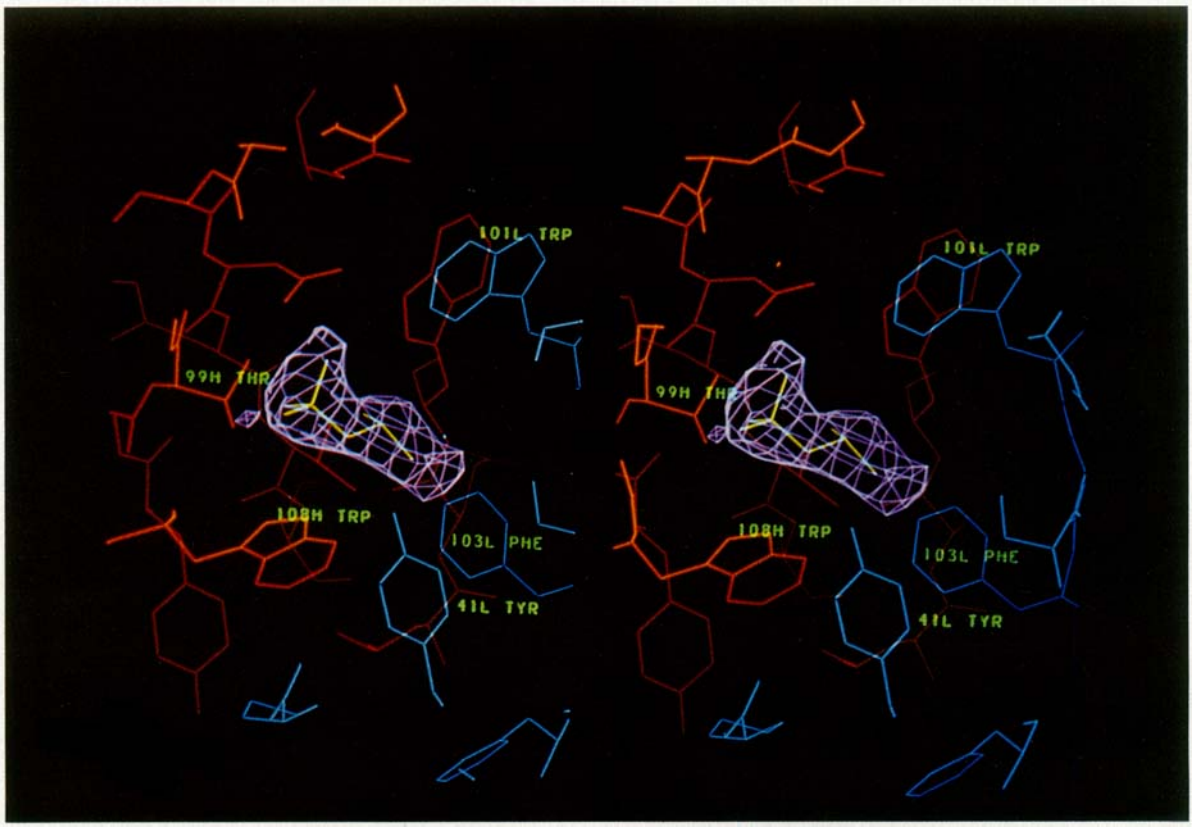

Fig. 7. Stereo diagram of the cage electron density (lavender) corresponding to a molecule of MPD in its binding site just below that of fluorescein in the V domain interface. Key residues of the light (blue) and heavy chains (red) are labeled with three-letter abbreviations. The hydroxyl groups of threonine H99 and tyrosine L41 may form hydrogen bonds with the 2-and 4-hydroxyl groups of MPD.

for fluorescein.[9] Figures 4 and 5 show a very tight fit of the ligand in the site, and the presence of tyrosine 102 and 103 further shields the bound ligand from additional reactants. These tyrosine residues are not present in the sequence of the 9-40 antibody, in which bound fluorescein is more accessible to iodide.[9]

The interactions of tyrosine L37 with fluorescein appear to be important in orienting the ligand in the high-affinity site. The stacking of the phenyl group of tyrosine with the xanthonyl ring was further stabilized by a hydrogen bond between the phenolic hydroxyl group and the phenylcarboxyl moiety of fluorescein. The dual interaction of fluorescein with tyrosine also played a major role in fixing the torsion angle between the xanthonyl and phenyl rings, which would have greater freedom to rotate in solution.

Studies of the effects of pH on lifetimes of dissociation indicated that ionizable groups ($pK > 8.0$) in the 4-4-20 active site contribute to the binding of fluorescein.[2] Lifetime maxima at pH 6.5–7.0 suggested that the xanthonyl moiety is negatively charged when bound to the 4-4-20 (the pK of the enolic group is 6.7[44]). In the 3-D structure of the complex the two enolic groups of fluorescein are bracketed by the ionizable side chains of histidine L31 and arginine L39. At the pH used for crystallization the histidine side chain would be expected to be in the uncharged form. The formation of an ion pair with arginine probably makes a very significant contribution to the binding energy, particularly in a region of low dielectric constant. In the 9-40 antibody this arginine is replaced by histidine,[41] a substitution that could partially account for the decrease in affinity relative to 4-4-20.

Rhodamine 110 and rhodamine B, structural analogs of fluorescein with amino (110) and diethylamino (B) groups substituted for the enolic oxygen atoms, do not bind to 4-4-20.[2] Acylamino groups

would have formal positive charges at relatively low pH values, (<5), at which there would be electrostatic repulsion by like charges on the histidine L31 and arginine L39 side chains. At pH 8 the only charge on a rhodamine molecule would reside on the phenylcarboxyl group. A monoanionic ligand would be incompatible with the pH profile of binding, which indicates a strong dependence on the presence of a dianion. In the case of rhodamine B, there is an additional steric factor to consider. For example, tetramethyl rhodamine formed a tight complex with the Mcg Bence–Jones dimer, but the tetraethyl derivative (rhodamine B) could not be accommodated in the binding site. Exposure to rhodamine B led to destruction of a crystal of the Mcg dimer in 5 hours.[13]

The crystal structure of the fluorescein–Mcg complex provides further insight into the minimal requirements for low-affinity binding of the ligand. As in 4-4-20, the ligand was accommodated in a network of aromatic residues. The xanthonyl ring of fluorescein was more deeply immersed in the cavity than the benzoyl moiety and participated in more interactions (14 vs 6) with the protein. A tyrosine side chain was wedged between the xanthonyl and benzoyl groups and largely dictated the torsion angle of 57° between these two rings. At the pH (6.2) of the crystals fluorescein was a monoanion and the charged group (phenylcarboxyl moiety) was oriented toward bulk solvent at the entrance of the binding cavity. In summary, the low-affinity site was more voluminous and there were fewer ligand–protein interactions. Aromatic rings did not stack, and potential negative charges were not balanced by basic side chains on the protein.

Thermodynamic studies indicated that the temperature stabilities of both the intact 4-4-20 antibody and Fab were significantly decreased in the presence of 40% (v/v) MPD.[5] These studies also suggested that the decrease in affinity for fluorescein in MPD was mainly attributable to conformational changes in the protein. Future comparisons of the present structure with that of the same complex crystallized in polyethylene glycol[5] will hopefully provide greater understanding of the general effects of these solvents.

Since MPD was added to the crystallization mixture after the formation of the hapten–Fab complex, we speculate that fluorescein would be dissociated from the protein prior to the admission of such a sizable solvent molecule to a deeper portion of the variable domain interface. Irrespective of the mode of entry of MPD, the local perturbations would be expected to have significant effects on the affinity constant of a hapten bound in a neighboring site.

ACKNOWLEDGMENTS

This article is dedicated to our late colleague, Martha Mason, who prepared the Fabs and crystals used in this work. We thank Kathryn Ely for advice and encouragement, Brad Nelson and Barbara Staker for photography and art work, Judy Baker for preparing the manuscript for publication, and Lynne Herron for aid in designing the graphics pictures. This work was supported by Grant CA 19616, awarded by the National Cancer Institute, Department of Health and Human Services (to A.B.E.), Grant AI 22898 (to J.N.H.), Grant AI 20960 (to E.W.V.), and N.I.H. Division of Research Resources Biomedical Research Grant RR07092 (to A.B.E.).

REFERENCES

1. Kranz, D.M., Voss, E.W., Jr. Partial elucidation of an antihapten repertoire in BALB/c mice: Comparative characterization of several monoclonal anti-fluorescyl antibodies. Mol. Immunol. 18:889–898, 1981.
2. Kranz, D.M., Herron, J.N., Voss, E.W., Jr. Ligand binding by monoclonal anti-fluorescyl antibodies. J. Biol. Chem. 257:6987–6995, 1982.
3. Herron, J.N. Equilibrium and kinetic methodology for the measurement of binding properties in monoclonal and polyclonal populations of antifluorescyl-IgG antibodies. In: "Fluorescein Hapten: An Immunological Probe." Voss, E.W., Jr., ed. Boca Raton, Florida: CRC Press, 1984:49–76.
4. Herron, J.N., Kranz, D.M., Jameson, D.M., Voss, E.W., Jr. Thermodynamic properties of ligand binding by monoclonal anti-fluorescyl antibodies. Biochemistry 25:4602–4609, 1986.
5. Gibson, A.L., Herron, J.N., He, X.-M., Patrick, V.A., Mason, M.L., Lin, J.-N., Kranz, D.M., Voss, E.W., Jr., Edmundson, A.B. Differences in crystal properties and ligand affinities of an antifluorescyl Fab (4-4-20) in two solvent systems. Proteins 3:155–160, 1988.
6. Voss, E.W., Jr., Eschenfeld, W., Root, R.T. Fluorescein: A complete antigenic group? Immunochemistry 13:447–453, 1976.
7. Kranz, D.M., Voss, E.W., Jr. Idiotypic analyses of monoclonal antifluorescyl antibodies. Location and characterization of idiotypic determinants. Mol. Immunol. 20:1301–1312, 1983.
8. Kranz, D.M., Ballard, D.W., Voss, E.W., Jr. Expression of defined idiotypes throughout the BALB/c anti-fluorescyl response: affinity and idiotype analysis of heterogeneous antibodies. Mol. Immunol. 20:1313–1322, 1983.
9. Bates, R.M., Ballard, D.W., Voss, E.W., Jr. Comparative properties of monoclonal antibodies comprising a high affinity anti-fluorescyl idiotype family. Mol. Immunol. 22: 871–877, 1985.
10. Amzel, L.M., Poljak, R.J., Saul, F., Varga, J.M., Richards, F.F. The three-dimensional structure of a combining region ligand complex of immunoglobulin NEW at 3.5 Å resolution. Proc. Natl. Acad. Sci. U.S.A. 71:1427–1430, 1974.
11. Segal, D.M., Padlan, E.A., Cohen, G.H., Rudikoff, S., Potter, M., Davies, D.R. The three-dimensional structure of a phosphorylcholine binding mouse immunoglobulin Fab and the nature of the antigen-binding site. Proc. Natl. Acad. Sci. U.S.A. 71:4298–4302, 1974.
12. Edmundson, A.B., Ely, K.R., Girling, R.L., Abola, E.E., Schiffer, M., Westholm, F.A., Fausch, M.D., Deutsch, H.F. Binding of 2,4-dinitrophenyl compounds and other small molecules to a crystalline λ-type Bence-Jones dimer. Biochemistry 13:3816–3827, 1974.
13. Edmundson, A.B., Ely, K.R., Herron, J.N. A search for site-filling ligands in the Mcg Bence-Jones dimer: Crystal binding studies of fluorescent compounds. Mol. Immunol. 21:561–576, 1984.
14. Edmundson, A.B., Ely, K.R. Binding of N-formylated chemotactic peptides in crystals of the Mcg light chain dimer: Similarities with neutrophil receptors. Mol. Immunol. 22:463–475, 1985.
15. Edmundson, A.B., Ely, K.R., Herron, J.N., Cheson, B.D. The binding of opioid peptides to the Mcg light chain dimer: Flexible keys and adjustable locks. Mol. Immunol. 24:915–935, 1987.

16. Amit, A.G., Mariuzza, R.A., Phillips, S.E.V., Poljak, R.J. Three-dimensional structure of an antigen-antibody complex at 2.8 Å resolution. Science 233:747–753, 1986.
17. Sheriff, S., Silverton, E.W., Padlan, E.A., Cohen, G.H., Smith-Gill, S.J., Finzel, B.C., Davies, D.R. Three-dimensional structure of an antibody-antigen complex. Proc. Natl. Acad. Sci. U.S.A. 84:8075–8079, 1987.
18. Tulloch, P.A., Colman, P.M., Davis, P.C., Laver, W.G., Webster, R.G., Air, G.M. Electron and x-ray diffraction studies of influenza neuraminidase complexed with monoclonal antibodies. J. Mol. Biol. 190:215–225, 1986.
19. Colman, P.M., Laver, W.G., Varghese, J.N., Baker, A.T., Tulloch, P.A., Air, G.M., Webster, R.G. Three-dimensional structure of a complex of antibody with influenza virus neuraminidase. Nature (London) 326:358–363, 1987.
20. Anderson, W.F., Cygler, M., Braun, R.P., Lee, J.S. Antibodies to DNA. Bio Essays 8:69–74, 1988.
21. Cygler, M., Boodhoo, A., Lee, J.S., Anderson, W.F. Crystallization and structure determination of an autoimmune antipoly (dT) immunoglobulin Fab fragment at 3.0 Å resolution. J. Biol. Chem. 262:643–648, 1987.
22. Herron, J.N., He, X.-M., Gibson, A.L., Voss, E.W., Jr., Edmundson, A.B. Crystal structure of a murine Fab fragment with specificity for single-stranded DNA. Fed. Proc. 46:2204, 1987.
23. Edmundson, A.B., Herron, J.N., Ely, K.R., He, X.-M., Harris, D.L., Voss, E.W., Jr. Synthetic site-directed ligands. Phil. Trans. Roy. Soc. Ser. B., in press.
24. Suh, S.W., Bhat, J.N., Navia, M.A., Cohen, G.H., Rao, D.N., Rudikoff, S., Davies, D.R. The galactan-binding immunoglobulin Fab J539: an x-ray diffraction study at 2.6-Å resolution. Proteins 1:74–80, 1986.
25. Bird, R.E., Hardman, K.D., Jacobson, J.W., Johnson, S., Kaufman, B.M., Lee S.-M., Lee, T., Pope, S.H., Riordan, G.S., Whitlow, M. Single-chain antigen-binding proteins. Science 242:423–426, 1988.
26. Gibson, A.L., Herron, J.N., Ballard, D.W., Voss, E.W., Jr., He, X.-M., Patrick, V.A., Edmundson, A.B. Crystallographic characterization of the Fab fragment of a monoclonal anti-ss-DNA antibody. Mol. Immunol. 22:499–502, 1985.
27. Rossmann, M.G., Blow, D.M. The detection of subunits within the crystallographic asymmetric unit. Acta Crystallogr. 15:24–31, 1962.
28. Crowther, R.A. Fast rotation function. In: "The Molecular Replacement Method: A Collection of Papers on the Use of Non-crystallographic Symmetry." Rossman, M.G., ed. New York: Gordon and Breach, 1972: 173–178.
29. Lattman, E.E., Love, W.E. A rotational search procedure for detecting a known molecule in a crystal. Acta Crystallogr. B26:1854–1857, 1970.
30. Fitzgerald, P.M.D. Merlot, an integrated package of computer programs for the determination of crystal structures by molecular replacement. J. Appl. Crystallogr. 21:273–278, 1988.
31. Herzberg, O., Sussman, J.L. Protein model building by the use of a constrained-restrained least-squares procedure. J. Appl. Crystallogr. 16:144–150, 1983.
32. Hendrickson, W.A. Stereochemically restrained refinement of macromolecular structures. In: "Methods in Enzymology." Wyckoff, H.W., Hirs, C.H.W., Timasheff, S.N., eds. Vol. 115, Orlando, Florida: Academic Press, 1985: 252–270.
33. Herron, J.N., He, X.-M., Voss, E.W., Jr., Edmundson, A.B. Structure of the Fab of an anti-ss-DNA autoantibody. Abstr. Protein Soc. S201, 1988.
34. Bedzyk, W.D., Johnson, L.S., Riordan, G.S., Voss, E.W., Jr. Variable region primary structure of a high affinity monoclonal anti-fluorescein antibody. J. Biol. Chem. 264:1565–1569, 1989.
35. Jones, T.A. A graphics model building and refinement system for macromolecules. J. Appl. Crystallogr. 11:268–272, 1978.
36. Pflugrath, J.W., Saper, M.A., Quiocho, F.A. New generation graphics system for molecular modeling. In: "Methods and Applications in Crystallographic Computing." Hall, S., Ashiaka, T., eds. Oxford: Clarendon Press, 1984: 404–407.
37. Connolly, M.L. Solvent-accessible surfaces of proteins and nucleic acids. Science 221:709–713, 1983.
38. Burley, S.K., Petsko, G.A. Aromatic-aromatic interaction: A mechanism of protein structure stabilization. Science 229:23–28, 1985.
39. Voss, E.W., Jr., Miklasz, S.D., Petrossian, A., Dombrink-Kurtzman, M.A. Polyclonal antibodies specific for liganded active site (metatype) of a high affinity antihapten monoclonal antibody. Mol. Immunol. 25:751–759, 1988.
40. Watt, R.M., Voss, E.W., Jr. Mechanism of quenching of fluorescein by anti-fluorescein IgG antibodies. Immunochemistry 14:533–541, 1977.
41. Bedzyk, W.D., Herron, J.N., Edmundson, A.B., Voss, E.W., Jr. Variable region primary structures of idiotypically cross-reactive anti-fluorescein monoclonal antibodies. FASEB J. ABS. 3:A1096, 1989.
42. Kranz, D.M., Herron, J.N., Giannis, D.E., Voss, E.W., Jr. Kinetics and mechanism of fluorescence enhancement due to deuterium oxide perturbation of fluorescyl ligand bound to purified homogeneous and heterogeneous antibodies. J. Biol. Chem. 256:4433–4438, 1981.
43. Watt, R.M., Voss, E.W., Jr. Solvent perturbation of the fluorescence of fluorescein bound to specific antibody. Fluorescence quenching of the bound fluorophore by iodide. J. Biol. Chem. 254:1684–1690, 1979.
44. Alexandru, I., Kells, D.I.C., Dorrington, K.J., Klein, M. Non-covalent association of heavy and light chains of human immunoglobulin G: studies using light chain labelled with a fluorescent probe. Mol. Immunol. 17:1351–1363, 1980.
45. Kabat, E.A., Wu, T.T., Reid-Miller, M., Perry, H.M., Gottesman, K.S. "Sequences of Proteins of Immunological Interest." U.S. Department of Health and Human Services, Public Health Service, National Institutes of Health, Bethesda, MD, 1987.